Spin-Resolved Tunneling Studies of the Exchange Field in EuS/Al Bilayers

Y. M. Xiong, S. Stadler, and P. W. Adams

Department of Physics and Astronomy, Louisiana State University, Baton Rouge, Louisiana 70803, USA

G. Catelani

Department of Physics, Yale University, New Haven, Connecticut 06520, USA
(Received 25 February 2011; published 14 June 2011)

We use spin-resolved electron tunneling to study the exchange field in the Al component of EuS/Al bilayers, in both the superconducting and normal-state phases of the Al. Contrary to expectation, we show that the exchange field H_{ex} is a nonlinear function of applied field, even in applied fields that are well beyond the EuS coercive field. Furthermore, the magnitude H_{ex} is unaffected by the superconducting phase. In addition, H_{ex} decreases significantly with increasing temperature in the temperature range of 0.1—1 K. We discuss these results in the context of recent theories of generalized spin-dependent boundary conditions at a superconductor-ferromagnet interface.

Owing to their different symmetries, itinerant ferromagnetic (FM) order and spin-singlet superconducting (SC) order are generally mutually exclusive. With rare exception, nature does not allow ferromagnetic order to coexist with BCS superconductivity [1]. This immiscibility can, however, lead to interesting effects in the vicinity of a FM-SC interface, as electrons moving from one region to the other try to accommodate the differing order parameters. Over the past decade significant progress has been made in understanding the nature of the SC order parameter in the proximity of a FM-SC interface [2–5]. In fact, much of the research on FM-SC structures has focused on the evanescent SC condensate residing on the FM side of the interface in properly prepared bilayers [4,6–8]. Remarkably, not only can SC Cooper pairs exist in the FM layer, but the exchange field in the FM induces a triplet component to the SC wave function [4]. This results in oscillations in the SC order parameter [5–7] that are reminiscent of the order parameter modulations predicted by Fulde and Ferrel [9] and Larkin and Ovchinnikov [10] for a BCS superconductor in a critical Zeeman field. In this Letter, we present the results of a detailed study of the exchange field induced in the SC side of a FM-SC bilayer. We show this proximity-induced exchange field is not static, but has unexpected temperature and applied-field dependencies that are not attributable to the temperature and/or field dependence of the FM magnetization.

Since we are primarily interested in the behavior of the exchange field induced in the SC layer, we have chosen an insulating material for the FM layer, EuS [11]. This greatly simplifies the interpretation of the data since electrons from the SC only enter the FM via evanescent wave functions. For the superconductor we chose Al since it has a very low spin-orbit scattering rate and its spin-paramagnetic phase diagram is well understood [12]. The FM-SC bilayers were fabricated by first depositing a 5-nm-thick EuS film via

e-beam evaporation onto fire-polished glass at 84 K. Then a 2.4-nm-thick Al film was deposited on top of the EuS film. The depositions were made at a rate of ~1 and ~0.1 nm/s, respectively, in a typical vacuum of $<3 \times 10^{-7}$ Torr. The samples were then exposed to air to form a native oxide on the Al surface. Finally, the bilayers where mechanically trimmed and a 10-nm-thick nonsuperconducting Al alloy counterelectrode (Al$_{ns}$) was deposited, with the native oxide serving as the tunnel barrier. The junction area was about 1 mm $\times$ 1 mm, while the junction resistance ranged from 15–100 KΩ depending on exposure time and other factors. Only junctions with resistances much greater than that of the films were used. At low temperature the tunneling conductance is proportional to the quasiparticle density of states (DOS) [13]. Measurements of resistance and tunneling were carried out on an Oxford dilution refrigerator using a standard ac four-probe technique. Magnetic fields of up to 9 T were applied using a superconducting solenoid. A mechanical rotator was employed to orient the sample *in situ* with a precision of ~0.1°.

The exchange field in both the SC and normal phases of the bilayers can be obtained via spin-resolved tunneling DOS measurements. For samples in the SC phase, we utilize the quasiparticle tunneling technique of Tedrow and Meservey [14]. This technique exploits the fact that the internal field in the SC film induces a Zeeman splitting of the DOS spectrum, resulting in the BCS coherence peaks being split into spin-up and spin-down bands. The separation of the bands, $\Delta V = E_z/e$ (with $E_z = 2\mu_B H_z$ the Zeeman energy), is a direct measure of the effective Zeeman field

$$H_z = \frac{H_{app} + H_{ex}}{1 + G_{eff}^0}, \tag{1}$$

where H_{app} is the applied field, H_{ex} the exchange field induced by the EuS interface, and G_{eff}^0 is the effective [15] antisymmetric Fermi liquid parameter. The latter accounts

for the renormalization of the electron spin by interactions. At low temperatures where $T \ll T_c$, $G_{eff}^0 \simeq 0$, whereas in the normal state $G_{eff}^0 = G_N^0$ with $G_N^0 \simeq 0.16$–0.26 [15].

In the upper panel of Fig. 1 we plot the 80 mK tunneling conductance of an EuS/Al-AlO$_x$-Al$_{ns}$ tunnel junction in an applied parallel magnetic field of $H_{app} = 0.03$ T. The Zeeman splitting of the BCS DOS spectrum is clearly evident. From this splitting we obtain $H_z \simeq 4.4$ T. When the Zeeman energy is of the order of the superconducting gap $\Delta_0 \sim 0.4$ mV the film undergoes a first-order transition to the normal state at the analog of the Clogston-Chandrasekhar critical field [16],
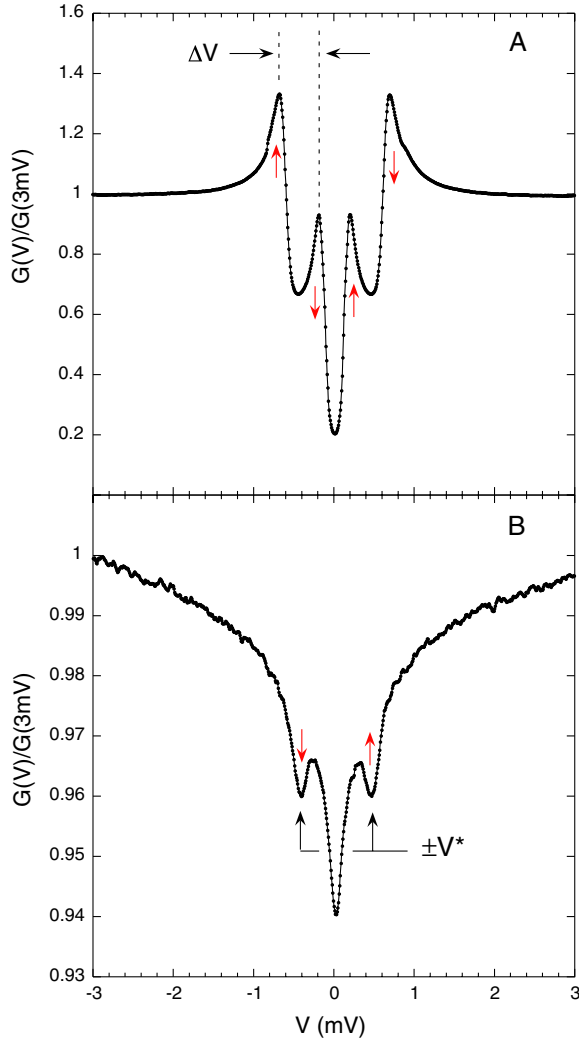

FIG. 1 (color online).   (a) Tunneling DOS spectrum in an applied parallel field of 0.03 T. The Zeeman splitting of the coherence peaks gives a direct measure of the Zeeman field. The gray (red) arrows denote the spin assignment of the coherence peaks. (b) Pauli-limited normal state in an applied parallel field of 0.1 T, where only the pairing resonance and the zero-bias anomaly remain. The Zeeman field can be extracted from the resonance energy V^* via Eq. (3). The gray (red) arrows denote the spin assignments of the occupied and unoccupied resonances.

$$H_z^c = \frac{\Delta_0}{\mu_B \sqrt{2(1 + G_N^0)}}. \qquad (2)$$

The parallel critical field in pristine Al films of comparable thickness to ones used in this study is $H_z^c \sim 6$ T [12]. For the film in Fig. 1 the transition to the normal state occurred at an applied field of only ~ 0.1 T. This is consistent with the tunneling data and indicates that the Zeeman field of the Al film was dominated by exchange. The magnitude of H_{ex} obtained from data such as that in Fig. 1 is comparable to that reported by Hao *et al.* who measured the magnitude of the exchange field as a function of Al thickness in the SC phase of EuS/Al bilayers [17]. Since the technique used in those early experiments required that the films be in the SC phase, the exchange fields could only be measured over a very narrow range of applied fields. As we discuss in detail below, by extending the measurements into the normal phase of the bilayers we are able to measure the exchange field over a much broader range of applied fields.

In the lower panel of Fig. 1 we plot the tunneling spectra of the same bilayer in an applied field of $H_{app} = 0.1$ T, which produced a Zeeman field exceeding H_z^c. The central dip in this normal-state spectrum is the *electron-electron* interaction zero-bias anomaly, which is independent of field [18,19]. The satellite features represent the pairing resonance, from which we can extract the Zeeman field [20,21]. The pairing resonance is spin assigned, as shown by the arrows in the figure. The energy of the resonance depends on the field via the Zeeman energy [20],

$$eV^* = \frac{1}{2}(E_z + \sqrt{E_z^2 - \Delta_0^2}). \qquad (3)$$

The positions of the resonances, as shown in the lower panel of Fig. 1, are obtained by first subtracting off the zero-bias anomaly background and then fitting the resonance profile, as described elsewhere [20]. We then use Eq. (3) to extract the Zeeman field.

In Fig. 2 we plot H_z as a function of a parallel field H_{app} at 80 and 400 mK for two different samples made under identical conditions. The 80 mK data set was obtained from both SC and normal-state tunneling spectra. This particular sample underwent a first-order transition to the normal state at an applied field of ~ 0.1 T. All of the 400 mK data points were obtained from normal-state spectra, since for this film $H_{ex} > H_z^c$ in zero applied field. There are several noteworthy features of these data. The first is that rather high internal fields can be achieved by applying fields of a few hundred G. The second is that there is a nonlinear increase in H_z between 0 and 2 T. We ascribe this behavior to a nonlinear dependence of the exchange field H_{ex} on H_{app}, as discussed below. Finally, H_z increases linearly in applied fields above 2 T, indicating a saturation of H_{ex} at high fields. The slope is determined by the Fermi liquid parameter G_N^0 as in Eq. (1). We can therefore obtain G_N^0 by fitting the data above 2 T to straight lines, as shown in Fig. 2. We find $G_N^0 = 0.19, 0.18$ for the 80 and 400 mK
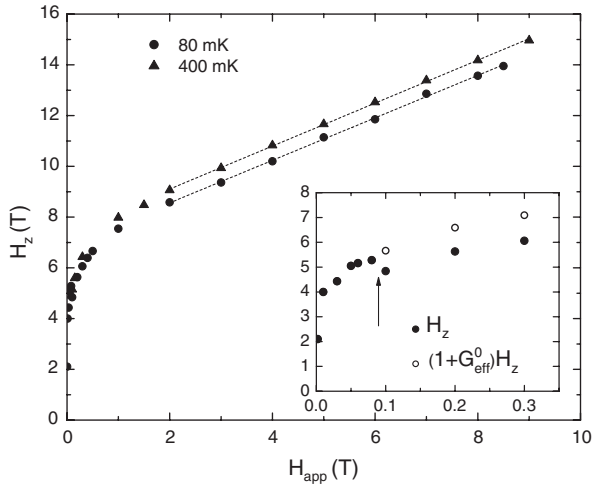
FIG. 2. Zeeman field [Eq. (1)] as a function of applied field. The dashed lines represent linear fits to the data above 2 T.

data sets, respectively, in good agreement with previously measured values in Al films [20].

As a check of the consistency of the above analysis, we show in the inset of Fig. 2 the Zeeman field versus H_{app} at 80 mK for low applied fields. The arrow points to the discontinuity in the Zeeman field at the critical field H_z^c. The discontinuity is caused by the jump of G_{eff}^0 from its SC value ($\simeq 0$) to its normal-state one. Indeed, H_z multiplied by $1 + G_{eff}^0$ evolves smoothly with applied field.

The exchange field can be extracted from the data in Fig. 2 by inverting Eq. (1). In Fig. 3 we show the resulting H_{ex} as a function of applied field at 80 and 400 mK. The arrow depicts the critical field transition in the 80 mK data set. Note that, below 2 T, H_{ex} grows nonlinearly with applied field, appearing to increase logarithmically by a
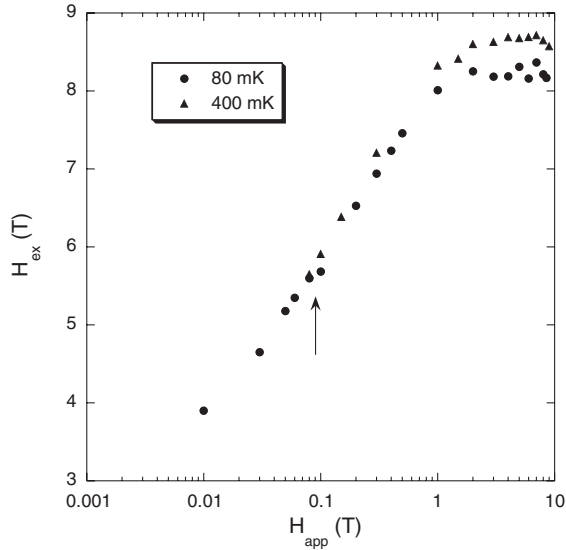

FIG. 3. Semilog plot of the EuS exchange field as a function of parallel applied field. The arrow denotes the superconducting critical field for the 80 mK data. All of the 400 mK were obtained from normal-state spectra.

factor of 2 between 0.01 and 1 T. Also, there is no obvious discontinuity in H_{ex} at the first-order transition. Similar enhancements in the exchange field with applied field were reported in both EuO/Al [22] and EuS/Al [17] bilayers. (Those measurements, however, were limited to the SC state, while here we are presenting results for the normal state as well.) This nonlinear behavior was attributed to the alignment of the ferromagnet domains by the applied field [14]. The authors argued that if the FM domains are randomly oriented on length scales on the order of the superconducting coherence length, then the average exchange field, as experienced by the SC, is lowered. In this scenario the applied field simply serves to align the domains. In order to explore this as a mechanism for the behavior in Fig. 3, we have directly measured the magnetization of the EuS/Al bilayers using a Quantum Design MPMS SQUID magnetometer.

In Fig. 4 we show the longitudinal magnetization, with field oriented along the film plane, of a stack of 10 EuS/Al bilayers at 2 K. The background magnetization of the glass slides was measured separately and subtracted from the raw data. Note that the magnetization loop is very sharp with a coercive field below 100 G. The saturation magnetization and Curie temperature are in good agreement with those of bulk EuS [11]. We find no evidence that the ferromagnetic behavior of the EuS has been significantly affected by its contact with the Al layer, as was conjectured in Ref. [23]. This suggests that observed increase in H_{ex} in applied fields between 0.01 and 2 T is not an artifact of domain alignment but is, in fact, an intrinsic effect.
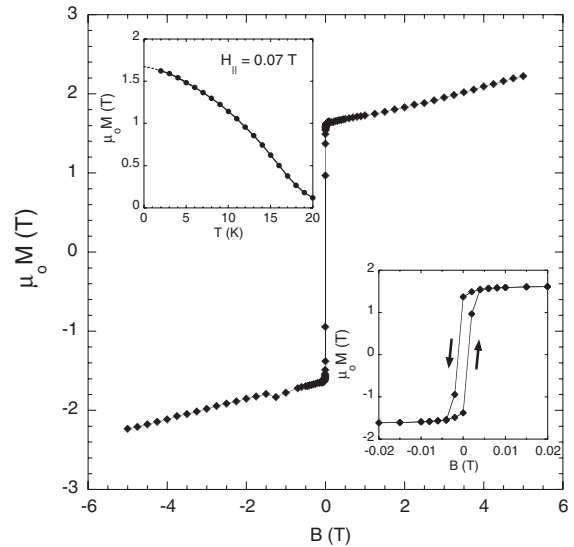

FIG. 4. Magnetization of a 5-nm-thick EuS film capped with 3 nm of Al. The external field was applied in the film plane. Lower inset is an expanded plot of the hysteresis loop. Note that the coercive field is less than 0.01 T. The upper inset is the temperature dependence of the magnetization in a 0.07 T parallel field. These data were taken after cycling the applied field to 5 T and back at 2 K. The dashed line in this inset is a polynomial fit to the data below 5 K.
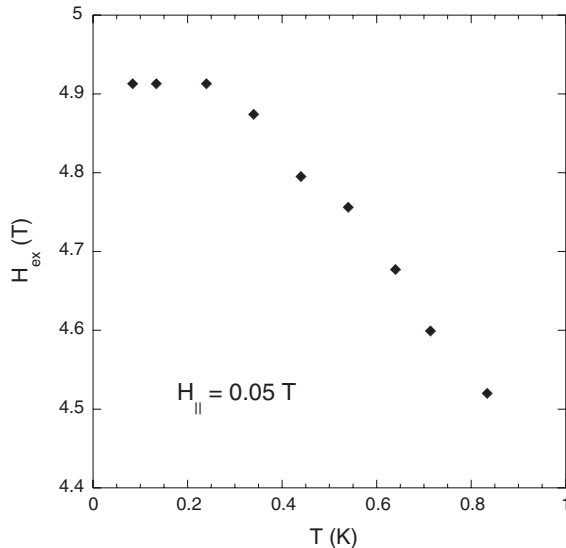
FIG. 5. Temperature dependence of the exchange field in a parallel applied field of 0.05 T.

Interestingly, H_{ex} also exhibits a significant temperature dependence below 1 K. In Fig. 5 we plot the exchange field as a function of temperature in the presence of a parallel applied field of $H_{app} = 0.05$ T. Note that the H_{ex} decreases by about 10% between 200 and 800 mK. The magnetization of the EuS below 2 K (see upper inset of Fig. 4) is only weakly temperature dependent and cannot explain the decrease H_{ex} with increasing temperature. This suggest that the behavior in Fig. 5 is a conduction-spin relaxation effect associated with thermally activated spin-flip scattering processes.

In the diffusive regime relevant to our Al films, the spin-dependent boundary conditions described in Refs. [7,8] should produce an exchange field that is determined solely by the properties of the EuS/Al interface and the normal-state properties of the Al films, such as their thickness and conductance. Consequently, the exchange field should, in fact, be insensitive to the phase of the Al film, which is the case for the EuS/Al bilayers in this study. Preliminary measurements show that a very similar, applied-field-dependent, exchange field arises in the Be component of EuS/Be bilayers [24]. In fact, this exchange field is evident even in samples with Be layers of sufficiently high resistance so as to be in the nonsuperconducting correlated insulator phase [25].

All of the current theoretical models treat the exchange field within the context of a superconducting ground state, and none of them can account for the fact that the exchange field is an intrinsic function of the applied field. If the underlying mechanism of this field dependence can be determined, then one would hope that the mechanism could be exploited in order to control the magnitude of the exchange field with substantially smaller external fields than used in this study. Or, perhaps, one may be able to modulate the interface exchange coupling with an external

electric field via a gate. In either case, the strategy is to use a small external field to control a large exchange field in order to realize a device, such as superconducting switch or a tunable polarized current source [26].

[1] S. Saxena et al., Nature (London) **406**, 587 (2000).
[2] A. I. Buzdin, L. N. Bulaevskii, and S. V. Panyukov, JETP Lett. **35**, 178 (1982).
[3] E. A. Demler, G. B. Arnold, and M. R. Beasley, Phys. Rev. **55**, 15 174 (1997).
[4] F. S. Bergeret, A. F. Volkov, and K. B. Efetov, Phys. Rev. Lett. **86**, 4096 (2001).
[5] T. Kontos, M. Aprili, J. Lesueur, and X. Grison, Phys. Rev. Lett. **86**, 304 (2001).
[6] A. Cottet and W. Belzig, Phys. Rev. B **72**, 180503 (2005).
[7] A. Cottet, Phys. Rev. B **76**, 224505 (2007).
[8] A. Cottet, D. Huertas-Hernando, W. Belzig, and Y. V. Nazarov, Phys. Rev. B **80**, 184511 (2009).
[9] P. Fulde and A. Ferrel, Phys. Rev. **135**, A550 (1964).
[10] A. I. Larkin and Y. N. Ovchinnikov, Sov. Phys. JETP **20**, 762 (1965).
[11] I. J. Guilaran, D. E. Read, R. L. Kallaher, P. Xiong, S. von Molnár, P. A. Stampe, R. J. Kennedy, and J. Keller, Phys. Rev. B **68**, 144424 (2003).
[12] V. Yu. Butko, P. W. Adams, and E. I. Meletis, Phys. Rev. Lett. **83**, 3725 (1999).
[13] M. Tinkham, Introduction to Superconductivity (McGraw-Hill, New York, 1996).
[14] P. M. Tedrow and R. Meservey, Phys. Rep. **238**, 173 (1994).
[15] G. Catelani, X. S. Wu, and P. W. Adams, Phys. Rev. B **78**, 104515 (2008).
[16] A. M. Clogston, Phys. Rev. Lett. **9**, 266 (1962); B. S. Chandrasekhar, Appl. Phys. Lett. **1**, 7 (1962).
[17] X. Hao, J. S. Moodera, and R. Meservey, Phys. Rev. Lett. **67**, 1342 (1991).
[18] B. L. Altshuler, A. G. Aronov, M. E. Gershenson, and Yu. V. Sharvin, Sov. Sci. Rev., Sect. A **9**, 223 (1987).
[19] Y. Imry and Z. Ovadyahu, Phys. Rev. Lett. **49**, 841 (1982).
[20] G. Catelani, Y. M. Xiong, X. S. Wu, and P. W. Adams, Phys. Rev. B **80**, 054512 (2009).
[21] Y. M. Xiong, P. W. Adams, and G. Catelani, Phys. Rev. Lett. **103**, 067009 (2009).
[22] P. M. Tedrow, J. E. Tkaczyk, and A. Kumar, Phys. Rev. Lett. **56**, 1746 (1986).
[23] T. Tokuyasu, J. A. Sauls, and D. Rainer, Phys. Rev. B **38**, 8823 (1988).
[24] Y. M. Xiong and P. W. Adams (to be published).
[25] V. Yu. Butko, J. F. DiTusa, and P. W. Adams, Phys. Rev. Lett. **85**, 162 (2000).
[26] F. Giazotto, F. Taddei, P. D'Amico, R. Fazio, and F. Beltram, Phys. Rev. B **76**, 184518 (2007).